JACS
JOURNAL OF THE AMERICAN CHEMICAL SOCIETY

ARTICLE

pubs.acs.org/JACS

Co_3O_4−SiO_2 Nanocomposite: A Very Active Catalyst for CO Oxidation with Unusual Catalytic Behavior

Chun-Jiang Jia,[†] Manfred Schwickardi,[†] Claudia Weidenthaler,[†] Wolfgang Schmidt,[†] Satu Korhonen,[‡] Bert M. Weckhuysen,[‡] and Ferdi Schüth*[,†]

[†]Max-Planck-Institut für Kohlenforschung, Kaiser-Wilhelm-Platz 1, 45470 Mülheim an der Ruhr, Germany

[‡]Inorganic Chemistry and Catalysis Group, Debye Institute for Nanomaterials Science, Faculty of Science, Utrecht University, 3584 CA Utrecht, The Netherlands

Supporting Information

ABSTRACT:

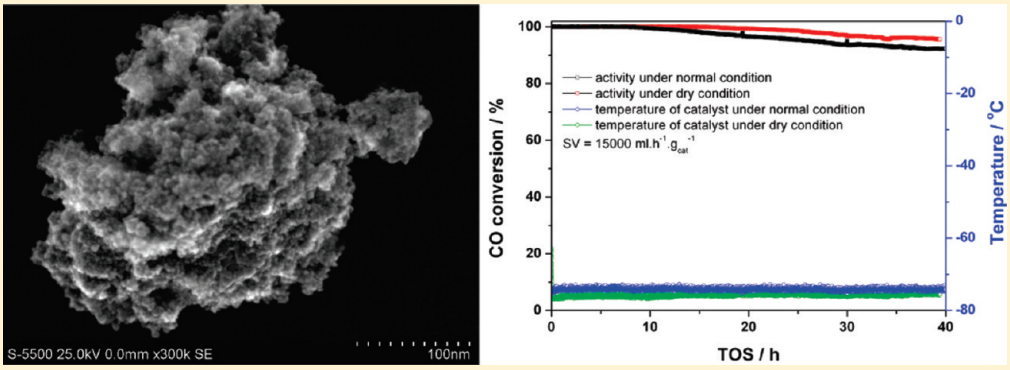

A high surface area Co_3O_4−SiO_2 nanocomposite catalyst has been prepared by use of activated carbon as template. The Co_3O_4−SiO_2 composite, the surface of which is rich in silica and Co(II) species compared with normal Co_3O_4, exhibited very high activity for CO oxidation even at a temperature as low as −76 °C. A rather unusual temperature-dependent activity curve, with the lowest conversion at about 80 °C, was observed with a normal feed gas (H_2O content ∼3 ppm). The U-shape of the activity curve indicates a negative apparent activation energy over a certain temperature range, which has rarely been observed for the heterogeneously catalyzed oxidation of CO. Careful investigation of the catalytic behavior of Co_3O_4−SiO_2 catalyst led to the conclusion that adsorption of H_2O molecules on the surface of the catalyst caused the unusual behavior. This conclusion was supported by in situ diffuse reflectance Fourier transform infrared (DRIFT) spectroscopic experiments under both normal and dry conditions.

INTRODUCTION

The heterogeneously catalyzed oxidation of carbon monoxide (CO) has been most extensively studied due to its relevance in practical applications, such as purification of air,[1] gas sensors for the detection of trace amounts of CO,[2] automotive exhaust gas treatment,[3] and polymer electrolyte fuel cells.[4] Meanwhile, CO oxidation is also used as a probe for the low-temperature activity of possible catalytic materials and as a model reaction for mechanistic studies.

The potential of supported gold nanoparticles as efficient catalysts for low-temperature reactions has aroused tremendous interest since the pioneering work of Haruta et al.[5] demonstrated high activity for CO oxidation of such particles deposited on various metal oxides. However, gold-based catalysts are very costly, and thus more cost-efficient alternatives with similar activity would be highly desirable. Some metal oxides, especially Co_3O_4,[6−10] are also known to be active for CO oxidation at ambient temperature but normally only in the absence of moisture. Low-temperature CO oxidation over Co_3O_4 has been intensively studied and different CO oxidation activities for Co_3O_4 in terms of light-off temperature, T_{50}, have been reported. Under dry conditions with moisture content below 1 ppm, Cunningham et al.[6] found a T_{50} of −54 °C for pure Co_3O_4 at a space velocity (SV) of 10 000 $mL \cdot h^{-1} \cdot g_{cat}^{-1}$. Thormählen et al.[11] reported a T_{50} of −63 °C for Co_3O_4 supported on Al_2O_3 with a normal feed gas at SV = 60 000 $mL \cdot h^{-1} \cdot g_{cat}^{-1}$. Recently, Co_3O_4 nanorods with predominantly exposed {110} faces[12] have been found to exhibit very high activity for CO oxidation at −77 °C at a SV of 15 000 $mL \cdot h^{-1} \cdot g_{cat}^{-1}$ under normal conditions. This led to the idea of preparing active catalyst through morphology-controlled synthesis, which ensures that specifically active faces are predominantly exposed at the surface. In most cases, however, it is difficult to prepare well-shaped solid catalysts that have such

Received: March 30, 2011
Published: June 22, 2011

dx.doi.org/10.1021/ja2028926 | J. Am. Chem. Soc. 2011, 133, 11279–11288

preferentially exposed active faces, and the morphologies obtained are often not stable under reaction conditions, especially at high temperature. On the other hand, very small particles without specific morphology can also be very active catalysts because a high absolute number of active sites are exposed, although the catalytically active faces may not be dominant for the whole surface. In previous work, we have used nanocast mesoporous Co_3O_4 as catalyst for CO oxidation, but only moderate activity was observed.[13] However, due to the interest in highly active catalysts for CO oxidation, the synthesis of small-sized Co_3O_4 particles with high activity for low-temperature reactions remained an interesting challenge.

In this paper, we report a two-step method for the preparation of a $Co_3O_4-SiO_2$ nanocomposite catalyst that exhibits very high activity for CO oxidation even at a temperature as low as −76 °C with normal feed gas. Under normal conditions, a U-shape was observed for the temperature-dependent activity curve, showing the existence of negative apparent activation energies. This has never been observed in CO oxidation catalyzed by metal oxides. Investigations on the catalytic behavior of $Co_3O_4-SiO_2$ catalyst under normal and dry conditions showed that adsorption of H_2O molecules on the surface of the catalyst is the origin of the abnormal catalytic behavior. These studies on the CO oxidation over small-sized $Co_3O_4-SiO_2$ material may open up new routes in the search for highly active catalysts and increase the knowledge on unusual temperature dependence of rates in heterogeneous catalysis.

EXPERIMENTAL SECTION

Catalyst Synthesis. The $Co_3O_4-SiO_2$ nanocomposite catalyst was prepared by a two-step method. For the first step, 6 g of activated carbon (Kugelkohle, Code R 1407, CarboTech GmbH) was impregnated under magnetic stirring with 1.588 mL of tetraethoxysilane (TEOS, 7.13 mmol) diluted with 2.2 mL of 99% ethanol. The solution was completely absorbed by the activated carbon in 5 min under continuous stirring. Then the composite material was transferred into a muffle oven and annealed (heating rate 4.5 °C·min^{-1}) at 350 °C for 30 min in air. During the heating process, the activated carbon was stable and no burn-off was observed. Black solid powder (6.54 g, $C-SiO_2$) was collected after the annealing process.

For the second step, the above $C-SiO_2$ composite material was added to 3.80 mL of aqueous $Co(NO_3)_2$ solution (3.75 M) under magnetic stirring. The $Co(NO_3)_2$ solution was completely absorbed by the $C-SiO_2$ composite material during intensive stirring for 15 min. The resulting solid was transferred into a muffle oven and calcined at 550 °C (heating rate 4.5 °C·min^{-1}) for 90 min in air. This calcination led to combustion of the activated carbon matrix, and 1.46 g of $Co_3O_4-SiO_2$ composite (molar ratio of Co:Si is 2:1) material was obtained. Before use in catalytic experiments, the $Co_3O_4-SiO_2$ powder was pressed, crushed, and sieved to 20−40 mesh.

Characterization. The powder X-ray diffraction (XRD) patterns were recorded on a Stoe STADI P diffractometer operating in reflection mode with Cu Kα radiation that was monochromatized with a secondary graphite monochromator. The nitrogen sorption measurements were performed on an ASAP 2010 unit (Micromeritics) at 77 K after activation at 200 °C for 4 h under vacuum. High-resolution scanning electron microscope (HR-SEM) images, scanning transmission electron microscope (STEM) images, and element mapping images, based on the energy-dispersive X-ray analysis (EDS) of the catalyst, were taken on a Hitachi S-5500 ultrahigh-resolution cold field emission scanning microscope at an acceleration voltage of 30 kV. Morphological and structural characterization of the catalysts was performed with a Hitachi HF2000 microscope equipped with a cold field emission gun at an acceleration voltage of 200 kV. X-ray photoelectron spectroscopy (XPS) measurements were performed with a Kratos HSi spectrometer with a hemispherical analyzer. The monochromatized Al X-ray source (E = 1486.6 eV) was operated at 15 kV and 15 mA. For narrow scans, an analyzer pass energy of 40 eV was applied. Hybrid mode was used as lens mode. The base pressure in the analysis chamber was 4×10^{-9} Torr. The binding energy scale was corrected for surface charging by use of the C 1s peak of contaminant carbon as reference at 285.0 eV.

In situ Raman measurements were carried out with a 785 nm laser and a power of 10−35 mW with a Kaiser Optical Systems Inc. Raman spectrometer. The sample was place in an in situ cell (Linkam 600) that could be heated to 500 °C and cooled to −100 °C. The sample was activated by heating to 360 °C with synthetic air (20 vol %/80 vol % mixture of O_2/N_2) at a gas flow rate of 100 mL/min. After dwelling for 30 min at that temperature, the sample was first cooled to room temperature, after which it was further cooled to −50 °C. Raman spectra were measured prior to activation, during heat treatment, after heat treatment, and at −50 °C under synthetic air. At −50 °C the sample was also exposed to CO (10% CO/He, 100 mL/min).

Fourier transform infrared (FTIR) spectra were measured in a diffuse reflectance cell (Harrick system) equipped with CaF_2 windows on a Nicolet Magna 560 FTIR spectrometer using a mercury−cadmium−telluride (MCT)/A detector with a spectral resolution of 4 cm^{-1}. After pretreatment of the catalysts (15 mg) in a gas flow of synthetic air (30 mL·min^{-1}) at 360 °C for 1 h, the reaction cell was cooled down to the desired temperature. Then a background spectrum was collected from the sample via 256 scans at 4 cm^{-1} resolution. The catalyst was exposed to reaction gas (1 vol % CO, 20 vol % O_2, 79 vol % N_2) with a flow rate of 30 mL·min^{-1}, and diffuse reflectance Fourier transform infrared (DRIFT) spectra were obtained by subtracting the background spectrum from subsequent spectra. These difference spectra are reported herein. For measurements under dry conditions, the feed gas was passed through a molecular sieve trap cooled to −78 °C (2-propanol/dry ice bath) before going into the reactor.

Catalytic Testing. The activities of catalysts for CO oxidation were measured in a plug flow reactor by use of defined amounts of catalyst (50 mg of catalyst, SV = 60 000 mL·h^{-1}·g_{cat}^{-1}; or 200 mg of catalyst, SV = 15 000 mL·h^{-1}·g_{cat}^{-1}) in a gas mixture of 1 vol % CO in air (1 vol % CO, 20 vol % O_2, and 79 vol % N_2, from Air Liquide, 99.997% purity, H_2O content ∼3 ppm) at a flow rate of 50 mL·min^{-1}. The operation temperature was controlled with a thermocouple and could be adjusted in the range of −100 to 400 °C. Temperatures measured during the catalytic tests are always referred to the value measured with a second thermocouple placed in the catalyst bed. Before measurement, the catalysts were first activated in situ in the synthetic air (20 vol % O_2/80 vol % N_2 mixture, from Air Liquide, 99.999% purity, H_2O content ∼3 ppm) or N_2 (from Air Liquide, 99.999% purity, H_2O content ∼3 ppm) at 360 °C for 60 min or activated in a gas mixture consisting of 5 vol % H_2 in N_2 (from Air Liquide, 99.999% purity, H_2O content 3 ppm) at 135 °C for 60 min with a flow rate of 50 mL·min^{-1}.

For a typical light-off run, in which the temperature was ramped, the reactor was cooled to −75 or −50 °C prior to each experiment under a flow of N_2 gas, which was then replaced by the reaction gas, after the base temperature had been reached. Then, the temperature was ramped with a rate of 2 °C·min^{-1} to the final temperature. The concentrations of CO_2 and CO were analyzed at the outlet of the reactor with nondispersive IR spectroscopy on two URAS 3E analyzers (Hartmann and Braun).

In a typical steady-state experiment, the system was adjusted to the desired temperature under N_2 flow, which was then replaced by the reaction mixture. The activity was recorded during the whole deactivation process.

The titration experiments were carried out in the same reactor in which the CO oxidation activities were tested, with 40 mg of catalyst.

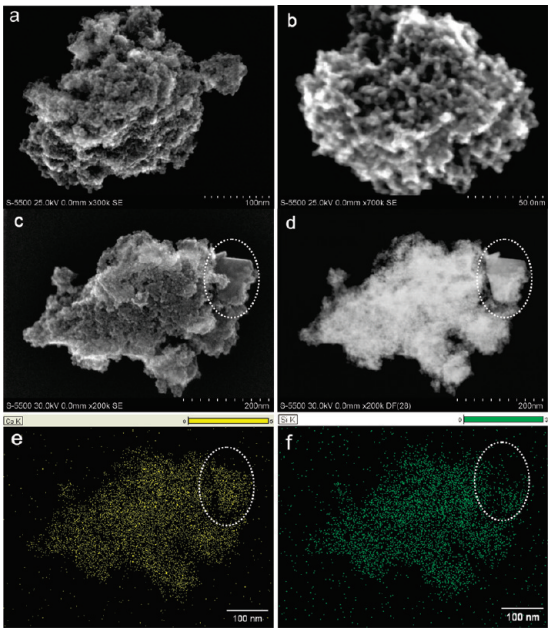

Figure 1. (a–c) SEM images, (d) dark-field STEM image (which corresponds to panel c), and (e, f) selected area element mapping images based on the EDS result (which also correspond to panel c) for the Co_3O_4–SiO_2 composite. The big particle shown in panels c and d is marked with white dotted circles. The Si mapping image in panel f shows that there is almost no Si signal for the upper half of this big particle, and the Si signal in the lower half comes from the small Co_3O_4–SiO_2 particles on the surface of the big particle, which is clearly shown in the STEM image of panel d. Based on the EDS result, the ratio of Co to Si is 1.9:1, which is almost the same as the ratio used for the synthesis.

The catalysts that had been pretreated in situ were cooled down to the desired temperature and kept in N_2 flow (67 mL·min^{-1}), and then they were further treated in a synthetic air flow (67 mL·min^{-1}) for 10 min. The catalysts were flushed with a N_2 flow to remove the O_2 gas from the reactor. After 10 min, the catalysts were exposed to a stream of 1% CO in N_2 (from Air Liquide, 99.997% purity, H_2O content ~3 ppm) at a flow rate of 67 mL·min^{-1} at the desired temperature. Online analysis was performed with a nondispersive IR analyzer (URAS 3E), that allowed detection of CO and CO_2 in a nitrogen matrix without interference problems.

For the experiments under dry conditions, the entire feed gases passed through a molecular sieve trap cooled to −78 °C (2-propanol/dry ice bath) before going into the reactor.

RESULTS AND DISCUSSION

The Co_3O_4–SiO_2 nanocomposite catalyst was synthesized by a two-step method using activated carbon spheres as exotemplate.[14] XRD investigation showed that only Co_3O_4 spinel is present as crystalline phase in the resulting composite (see Figure S1, Supporting Information). No shift of diffraction peaks was observed with respect to conventional Co_3O_4 spinel (PDF-2 entry 42-1467), indicating that no silicon-containing solid solution was formed. Silicon is most probably present as amorphous SiO_2 next to the spinel phase. Nitrogen sorption isotherms (Figure S2, Supporting Information) revealed that the Co_3O_4–SiO_2 composite is mesoporous with a Brunauer–Emmett–Teller (BET) surface area of about 210 m^2·g^{-1} and a pore volume of 0.20 cm^3·g^{-1}. From SEM images (Figure 1), it is seen that the product consists mainly of small uniform nanoparticles with sizes

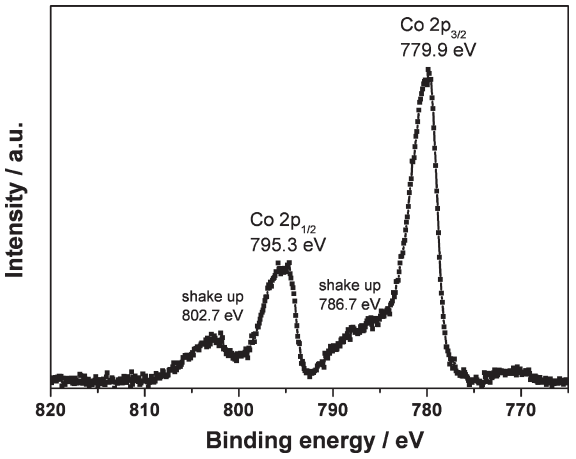

Figure 2. Co 2p photo peaks for fresh Co_3O_4–SiO_2 catalyst. The obvious shakeup satellite at ca. 786.7 eV indicates a high abundance of Co(II) species on the surface of the catalyst.

ranging from 5 to 10 nm. Aggregation of the small primary particles causes textural porosity as shown in Figure 1b, which corresponds well to the sorption data. It is noteworthy that, besides small particles, trace amounts of particles bigger than 50 nm were also observed. This can be clearly seen in the SEM and STEM images (Figure 1c,d). The selected area element (Co and Si) mapping images (Figure 1e,f) demonstrate that Co and Si are more or less uniformly dispersed for the small Co_3O_4–SiO_2 composite particles; no obvious Co-rich or Si-rich region was observed. However, the bigger particle marked with a circle in Figure 1c,d is basically a pure cobalt oxide particle without traces of silica. The difference in distribution of Co and Si in smaller and bigger particles indicates that the presence of Si directly influenced the particle size of the Co_3O_4 spinel; that is, the composite of Co_3O_4–SiO_2 is small-sized, whereas pure Co_3O_4 tends to form bigger particles. Particle size and porosity of Co_3O_4–SiO_2 strongly depend on the ratio of Co to Si. The results of a detailed study on this issue will be reported elsewhere.

To provide further insight into the microstructure of the Co_3O_4–SiO_2 catalyst, TEM investigations were also performed. Typical TEM images are shown in Figure S3 (Supporting Information). For the small particles with sizes of 5–10 nm, each individual comprises a single crystalline domain. Lattice fringes, as shown in Figure S3c (Supporting Information), indicate *d* values of 0.33 and 0.59 nm, which correspond to the (−112) and (110) lattice planes of Co_3O_4. The corresponding HRTEM images of larger 100 nm particles show that they also comprise single crystalline domains of Co_3O_4 spinel. It is noteworthy that no amorphous particles or surface layers of SiO_2 on the Co_3O_4 particles were observed on TEM images. XPS characterization was performed to investigate the surface composition and chemical state of the catalyst. The Co $2p_{3/2}$ and $2p_{1/2}$ peak positions (Figure 2) are in accord with the presence of Co_3O_4.[15] However, the obvious shakeup satellite at about 786.7 eV, which is an intermediate value compared with that for CoO (at 785 eV) and Co_3O_4 (at 789 eV), indicates a high abundance of Co(II) species on the surface of the catalyst compared with normal Co_3O_4 (see Figure S4a, Supporting Information). Based on the quantitative XPS result, the molar ratio of Si to Co is roughly 1, which is much higher than that observed from bulk EDX analysis (1:1.9), confirming that most of the SiO_2 is on the surface of the catalyst.

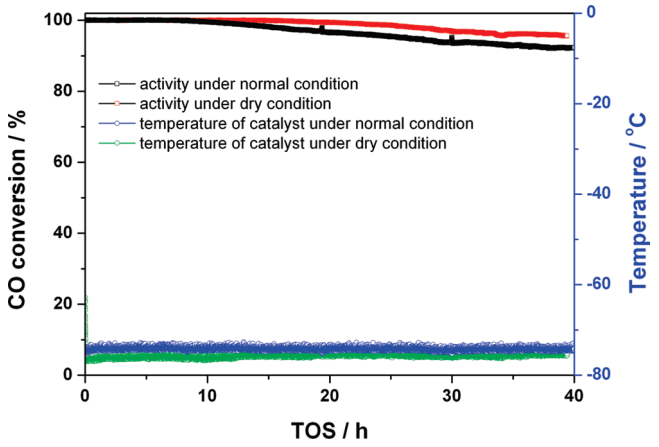

Figure 3. Catalytic performance of the $Co_3O_4-SiO_2$ catalyst for CO oxidation at a constant temperature of −76 °C for 40 h under both normal and dry conditions. Catalyst, 200 mg; reaction gas flow rate, 50 mL·min^{-1}; SV = 15 000 mL·h^{-1}·g_{cat}^{-1}.

The $Co_3O_4-SiO_2$ nanocomposite was tested for CO oxidation at −76 °C under constant conditions (SV 15 000 mL·h^{-1}·g_{cat}^{-1}). Under these conditions, it showed full conversion of CO to CO_2 during the initial 10 h; the CO conversion then decreased slightly but was still higher than 92% after 40 h (Figure 3, black curve). This catalyst thus performs at least as well as the specially designed catalyst with the rod morphology described in ref 12. The spent catalyst can be fully regenerated after that deactivation process through calcination in synthetic air at 360 °C for 1 h. The particle sizes and chemical state of the used catalyst were identical to those of the fresh one (see Figures S4−S6, Supporting Information). This indicates that the $Co_3O_4-SiO_2$ catalyst is very stable during the CO oxidation process. It is known that Co_3O_4 is sensitive to moisture in the feed gas.[6,16] For comparison, we therefore also measured the catalytic activity of the catalyst under dry conditions. Surprisingly, the catalytic performance was almost identical under normal and dry conditions.

Generally, Co(III) on the catalyst surface is thought to provide the active sites for CO oxidation and Co(II) is considered as inactive.[10] However, the $Co_3O_4-SiO_2$ nanocomposite, the surface of which is rich in silica and Co(II) species compared with normal Co_3O_4, also shows exceedingly high activity, which may suggest that Co(III) is not the only active species for CO oxidation. However, this needs to be studied more closely in the future. In any case, this catalyst appears to be highly attractive for low-temperature CO oxidation and outperforms other metal oxides reported so far[6−12,17,18] and even gold catalysts.[19]

For most catalysts for CO oxidation, based on supported gold or metal oxides, the activity increases with increasing reaction temperature. However, a very different temperature-dependent activity behavior was observed for the $Co_3O_4-SiO_2$ catalyst in the temperature range of −75 to 300 °C as shown in Figure 4a. Before the catalytic activity test with SV = 60 000 mL·h^{-1}·g_{cat}^{-1}, the catalyst was pretreated in situ in synthetic air. At temperatures from −75 to −50 °C, the activity for CO oxidation increases with increasing temperature; then the activity curve shows a U shape. The catalyst shows full conversion at the given space velocity at temperatures from −50 to 35 °C and above 160 °C, but in the temperature range of 35−160 °C the conversion rapidly decreases to a minimum at a temperature of about 80 °C and then successively increases again to full conversion. Such a complex U-shaped

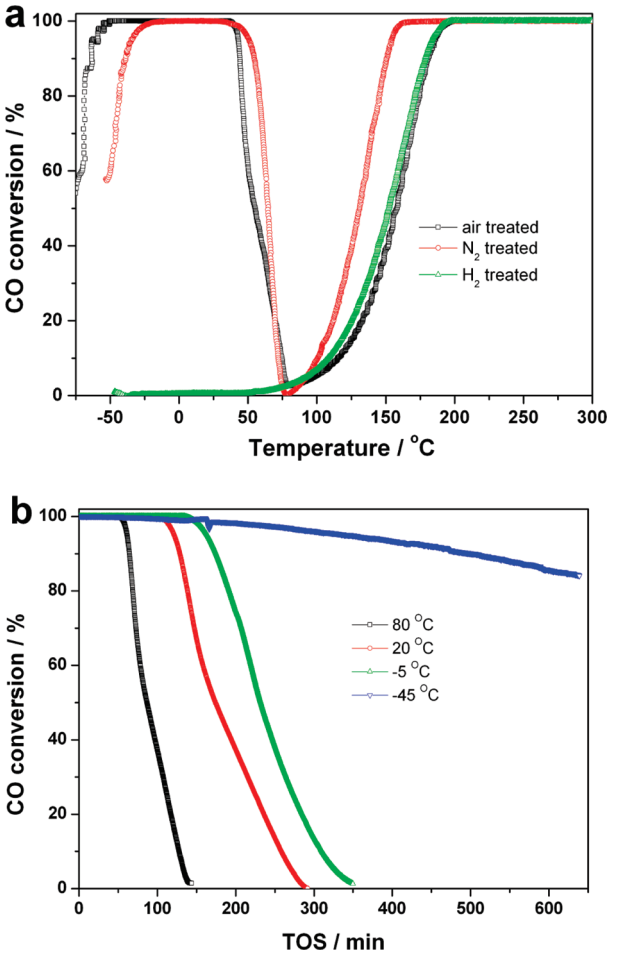

Figure 4. (a) Temperature dependence of the activity for CO oxidation for variously pretreated $Co_3O_4-SiO_2$ catalysts, and (b) catalytic performance of the catalyst pretreated in synthetic air at constant temperatures of −45, −5, 20, and 80 °C. All the above experiments were carried out under normal conditions. Catalyst, 50 mg; reaction gas flow rate, 50 mL·min^{-1}; SV = 60 000 mL·h^{-1}·g_{cat}^{-1}.

curve indicates the existence of negative apparent activation energy. Negative apparent activation energies have occasionally been observed in heterogeneous catalysis. The apparent activation energy is a composite of the activation energy of the surface reaction and adsorption enthalpies, which can result in negative apparent energies over certain temperature ranges. Such a phenomenon has been observed before in CO oxidation, for example, for $Au/Mg(OH)_2$[20,21] and Au/MgO[21] catalysts. Cunningham et al.[20] attributed the negative apparent activation energy over $Au/Mg(OH)_2$ to the direct interaction of CO with hydroxyl radicals present at the interface between the gold and $Mg(OH)_2$, but no additional evidence was provided. Recently, we reported similar catalytic behavior using both $Au/Mg(OH)_2$ and Au/MgO as catalysts for CO oxidation.[21] The experimental results suggest that the reaction proceeds via two different oxygen species, a highly active species at low temperature, the coverage of which decreases strongly in the temperature range over which the negative apparent activation energy is observed, and a less active species, which is oxidizing the CO at higher temperature and which shows the normal Arrhenius-type behavior. In order to explore whether the unusual conversion versus temperature curves observed in the present study are due to a

similar mechanism as over Au/MgO or Au/$Mg(OH)_2$, this effect was studied in more detail.

Light-off curves measured under transient conditions, as used here, may give misleading information, so activity tests under stationary conditions were performed at different temperatures, also with the aim to detect possible deactivation of the catalysts. The stability of the $Co_3O_4-SiO_2$ catalyst was tested at −45, −5, 20, and 80 °C. It was highly active and showed very stable CO oxidation at low temperatures (see Figure 4b). At −45 °C, the catalyst deactivated slightly and the CO conversion decreased by only 16% over more than 10 h. At −5 °C, full conversion of CO to CO_2 was observed up to 135 min, and then the conversion of CO decreased gradually to zero within 215 min. At 20 and 80 °C, full CO conversion was observed for even shorter times on stream and the succeeding deactivation of the catalyst was even faster. The CO conversion decreased from 100% to zero within 182 and 88 min at 20 and 80 °C, respectively. Overall, the results of the steady-state experiments are consistent with those of the light-off activity tests.

In addition to performing experiments in oxidative atmosphere, we also investigated the effect of inert (N_2) and reductive (5 vol % H_2 in N_2) pretreatment atmospheres on the activity of the $Co_3O_4-SiO_2$ catalyst. The catalyst pretreated with N_2 exhibited very similar behavior to that of the catalyst pretreated under oxidative atmosphere (see Figure 4a and Figure S7, Supporting Information). This was different for the catalyst pretreated under reductive atmosphere (5 vol % H_2 in N_2). A more or less normal temperature-dependent activity curve was observed; that is, no conversion was observed at temperatures below 50 °C and then, at temperatures above 50 °C, noticeable conversion was observed, which successively increased with increasing reaction temperature. Thus, the pretreatment significantly affects the catalytic performance of the catalyst. Oxidative and inert gas pretreatments are favorable, whereas reductive atmosphere leads to very low activity at lower temperature. While it is clear that inert or oxidative pretreatment leads to the formation of active catalysts at low reaction temperature, this does not reveal the reason for the unusual temperature dependence of the reaction rate.

It is known that the adsorption and activation of molecular oxygen are crucial for gold catalysts for CO oxidation.[22−26] The formation of adsorbed reactive oxygen species, such as superoxide ions (O_2^-), can be correlated to the presence of surface oxygen vacancies on the metal oxide support[24] or at the metal−support interfaces.[23−25] Different kinds of superoxide species have been reported to exist between −196 and 25 °C on the surfaces of CoO−MgO solid solutions,[27] and it was thus hypothesized that such superoxide species may play an important role in CO oxidation also over the system investigated here at low temperatures.[28,29] Therefore, CO titration experiments in the absence of oxygen (1 vol % CO in N_2) were also performed. This allows assessing the extent of the supply of oxygen stored on the catalyst. Figure 5 shows the transient response of CO_2 and CO evolution over differently pretreated $Co_3O_4-SiO_2$ catalysts at different temperatures. For the $Co_3O_4-SiO_2$ catalyst pretreated in synthetic air, the ability to provide reactive oxygen is rather high at low temperature (−45 °C). Strong CO_2 evolution with a maximum (CO_2 concentration 0.77%) at 100 s after exposure to CO was observed. The initial sharp CO_2 response is indicative of a fast reaction proceeding via rapid adsorption of CO, followed by reaction of the CO with reactive oxygen at the catalyst surface. It is noticed that, even after 1000 s, substantial amounts of CO_2 were still produced (CO_2 concentration 0.18%). At 20 °C, a CO_2

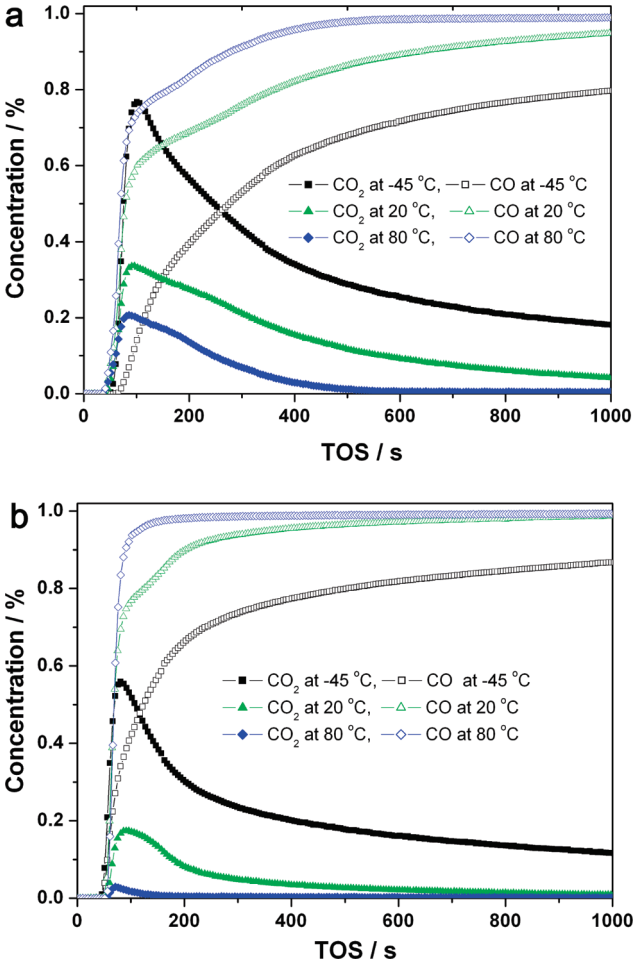

Figure 5. CO_2 response in CO titration experiments of the $Co_3O_4-SiO_2$ catalysts pretreated with (a) synthetic air and (b) N_2 at temperatures of −45, 20, and 80 °C. All the above experiments were carried out under normal conditions. Catalyst, 40 mg; reaction gas, 1 vol % CO in N_2; flow rate, 67 mL·min^{-1}.

response maximum was observed after 95 s, however, it was a lower concentration (0.34%) than that observed at −45 °C. The CO_2 evolution decreased gradually to 0.04% at TOS of 1000 s. At 80 °C, the CO_2 concentration peaked after 85 s (0.21%), and then it decreased to zero after 510 s. From the above results, it can be seen that the ability of the $Co_3O_4-SiO_2$ catalyst to supply reactive oxygen is substantially higher at −45 °C than at 20 and 80 °C, which corresponds well to the temperature dependence of the CO oxidation activity. Similar results for CO titration experiments were also obtained for $Co_3O_4-SiO_2$ pretreated in N_2. However, the corresponding maxima of the CO_2 responses of the catalyst pretreated in N_2 were weaker compared to those observed for catalysts pretreated in oxygen-containing atmosphere. For the catalyst pretreated in H_2, the ability to provide reactive oxygen is negligible at low temperature (−45 °C). However, it increases with increasing temperature (see Figure S8, Supporting Information), which is also consistent with the temperature dependence of the activity of catalysts pretreated in H_2.

The integral under the curves reported in Figure 5 allows calculation of the total amount of active oxygen on the surface of the catalyst. In order to estimate whether bulk oxygen contributes to the CO oxidation in the titration experiments, the

Table 1. Amount of Oxygen Consumed from Co_3O_4−SiO_2 Nanocomposite Catalysts in CO Titration Experiments[a,b]

temp, °C	pretreatment atmosphere	O consumption, mmol
	Normal Feed Gas	
−45	synthetic air	0.15
−45	N_2	0.092
20	synthetic air	0.061
20	N_2	0.018
80	synthetic air	0.021
80	N_2	0.0018
	Dry Feed Gas	
−45	synthetic air	0.20
−45	N_2	0.12
20	synthetic air	0.21
20	N_2	0.11
80	synthetic air	0.22
80	N_2	0.14

[a] Maximum surface oxygen (O^{2-}) capacity of the catalyst is 0.22 mmol. This capacity is calculated with the assumption that the surface of the catalyst is composed only of $(111)_{Co3O4}$; the detailed calculation process is shown in Figure S9, Supporting Information. [b] CO titration experiments are shown in Figures 5 and 7c,d.

maximum amount of oxygen that could be present just on the surface was calculated. This was done under the assumption that the surface does not contain SiO_2 and is only composed of the close-packed (111) plane of Co_3O_4. This corresponds to the highest amount of oxygen imaginable on the surface of the catalyst. For all the catalysts used in the CO titration experiments, the amounts of consumed oxygen are lower than this maximum amount (Table 1). However, considering that the surface of the catalyst most probably does not consist only of pure $(111)_{Co3O4}$ plane but also could expose $(110)_{Co3O4}$ or $(100)_{Co3O4}$, in which the oxygen density is lower than that of $(111)_{Co3O4}$, or could also expose amorphous SiO_2, the true amount of surface oxygen is probably lower than the ideally calculated value. Therefore, it is still possible that some framework oxygen from the bulk is involved during the CO titration process. For example, in the experiments with the catalyst pretreated with synthetic air for the CO titration at −45 °C, the calculated oxygen consumption in 1000 s is 0.15 mmol, which is only slightly smaller than the ideal maximum value (0.22 mmol), indicating the possibility of oxygen supply from the bulk of the catalyst.

On the basis of the above results, a depletion of active oxygen from the catalyst pretreated in synthetic air or N_2 with increasing temperature could be responsible for the negative apparent activation energy at intermediate temperatures. A high ability of the catalyst to supply reactive oxygen would be responsible for the remarkable activity in CO oxidation at low temperatures. Pretreatment of the catalyst in H_2 may, on the one hand, remove a substantial amount of surface oxygen. This would lead to low activity at low temperature, since no reactive oxygen could be provided for the CO oxidation. Alternatively, or in addition to this, the surface structure of the catalyst might be reconstructed by the treatment in H_2, which would diminish the ability of the catalyst for activation of the oxygen from the reaction gas.

In order to prove the validity of that hypothesis, complementary experiments were performed in order to detect certain reactive oxygen species on the catalyst surfaces. We used in situ

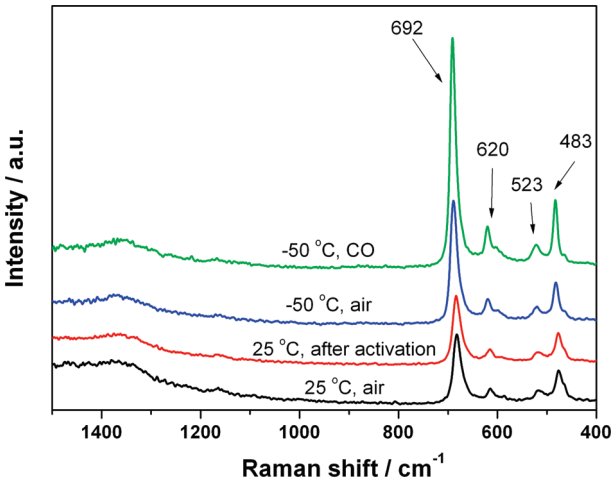

Figure 6. In situ Raman spectra of the Co_3O_4−SiO_2 catalyst under different conditions.

Raman spectroscopy, which has been reported by Corma and co-workers[24,25] as an effective technique to detect reactive oxygen species on surfaces of metal oxides. Figure 6 shows Raman spectra of samples measured under different conditions. No indication of reactive oxygen species of the peroxide or superoxide type could be found in these spectra. At room temperature, prior to heat treatment, only bands at 683, 618, 519, and 476 cm^{-1} were observed, which were assigned to Co_3O_4.[30] No features of peroxide or superoxide species, which are expected at about 1128 and 883 cm^{-1},[31,32] were observed during the heat treatment, cooling to −50 °C, or upon CO addition. Thus, peroxide and/or superoxide species are most likely not the origin of the unexpectedly high activity at low temperature or the unusual temperature dependence of the CO oxidation activity. Recently, Haruta and co-workers[7] proposed weakly bound oxygen species, such as bridged Co^{3+}−O_2^-−Co^{2+} (adsorbed molecular oxygen anion) and Co^{3+}−O^-−Co^{2+} (adsorbed atomic oxygen anion), as reactive oxygen species for a Co_3O_4 catalyst that exhibits high reactivity toward adsorbed CO species to form CO_2 even at −80 °C. However, no spectroscopic evidence of these reactive oxygen species (Co^{3+}−O_2^-−Co^{2+} and Co^{3+}−O^-−Co^{2+}) was provided, and no in situ characterization techniques were used to detect the formation of these possible species. For the catalyst system studied in this work, we cannot explain, how the low-temperature reactive oxygen species is formed and also have no indication of its nature, beyond the exclusion of some types of oxygen, as discussed above. The precise identification of reactive oxygen species involved in the oxidation of CO over the Co_3O_4−SiO_2 catalyst is still an open task.

As mentioned above, Co_3O_4 is intrinsically active for CO oxidation under dry conditions (H_2O concentration ≤1 ppm). However, in normal feed gas, active sites of Co_3O_4 can be covered by adsorbed H_2O, so that the adsorption of CO and oxygen is substantially hindered. As shown in Figure 3, there is almost no activity difference in CO oxidation at −76 °C under normal and dry conditions. However, at such low temperature, the partial pressure of water vapor is very low (about 0.0004 Torr at −80 °C,[33] corresponding to 0.5 ppm), since moisture present in the feed may freeze out before the catalyst bed, which in turn would reduce the extent of H_2O adsorption on active sites on the surface of the catalyst. However, at moderate temperatures the

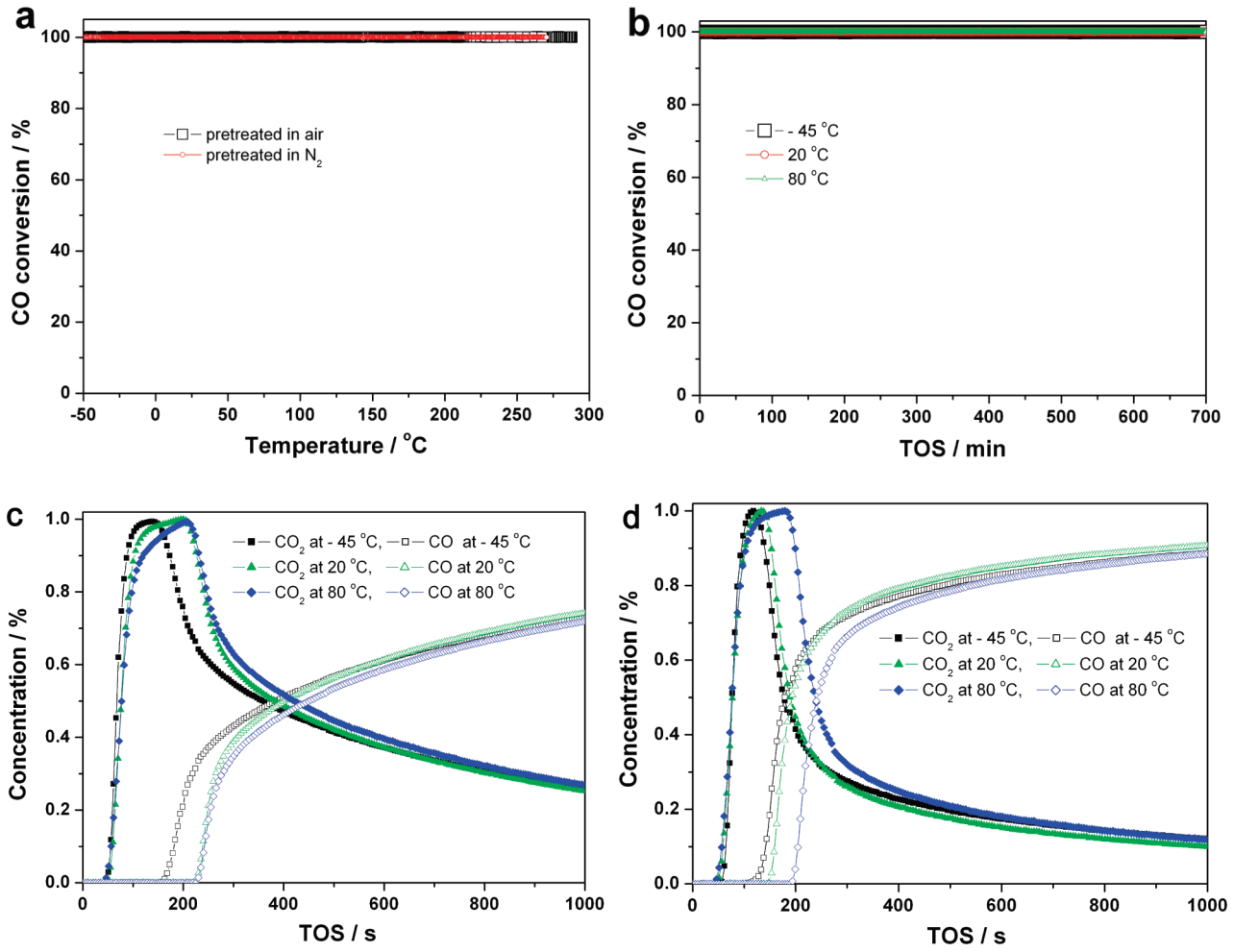

Figure 7. (a) Temperature dependence of activity for CO oxidation of $Co_3O_4-SiO_2$ catalysts. (b) Catalytic performance of catalyst pretreated with synthetic air at constant temperatures of −45, 20, and 80 °C. (c, d) CO_2 response in CO titration experiments of $Co_3O_4-SiO_2$ catalysts pretreated with (c) synthetic air and (d) N_2 at constant temperatures of −45, 20, and 80 °C. All the above experiments were carried out under dry conditions. For CO oxidation test, catalyst = 50 mg and reaction gas flow rate = 50 mL·min^{-1}; for CO titration test, catalyst = 40 mg, reaction gas = 1 vol % CO in N_2, and flow rate = 67 mL·min^{-1}.

catalyst will experience the water vapor pressure of the feed gas. Under these conditions, H_2O could compete with the reaction gases for active sites, resulting in reduced activity. Thus, water adsorption could be the origin of the unusual activity versus temperature curve. To check this hypothesis, we performed CO oxidation and CO titration tests with the $Co_3O_4-SiO_2$ catalyst under dry conditions (gas passed through a molecular sieve trap cooled to −78 °C via a 2-propanol/dry ice bath). Figure 7 panels a and b show the activity for CO oxidation measured under transient and steady-state conditions, respectively. The light-off experiments show that full conversion of CO to CO_2 is now maintained during the heating process in the temperature range from −50 to 300 °C. The U-shaped temperature-dependent activity discussed above was no longer observed. We further investigated the long-term stability of the catalyst at different temperatures under dry conditions, the results of which are shown in Figure 7b. Irrespective of the temperature regime of the experiments, the catalyst always gave full conversion of CO. For CO titration experiments under dry conditions (see Figure 7c,d), it was observed that the signal of the CO_2 response was much higher than that recorded under normal conditions, indicating that the ability of the catalyst to provide reactive oxygen is greatly enhanced in the absence of moisture. The total amount of oxygen of the catalyst involved in the CO titration under dry conditions was also calculated, the results of which are shown in Table 1. It is noticed that for the catalysts pretreated in synthetic air, the amounts of oxygen consumed in the CO titration at 20 and 80 °C are almost identical to the ideally calculated maximum values, which indicates that framework oxygen from the bulk of the catalyst most probably participates in the oxidation of CO during the CO titration. Moreover, in contrast to the experiment with the undried feed gas, stronger evolution of CO_2 was obtained at higher temperatures. All the results of the experiments under normal and dry conditions suggest that the moisture of the feed gas plays a major role and that competitive water adsorption is the origin of the U-shaped temperature-dependent activity.

To better understand the origin of the different catalytic behavior under normal and dry conditions, we studied the adsorbed species on the catalysts by in situ DRIFT spectroscopy, which can provide valuable insight into the mechanism of heterogeneous catalytic reactions, especially under in situ conditions.[34,35] Here, DRIFT spectra were collected to gain direct information

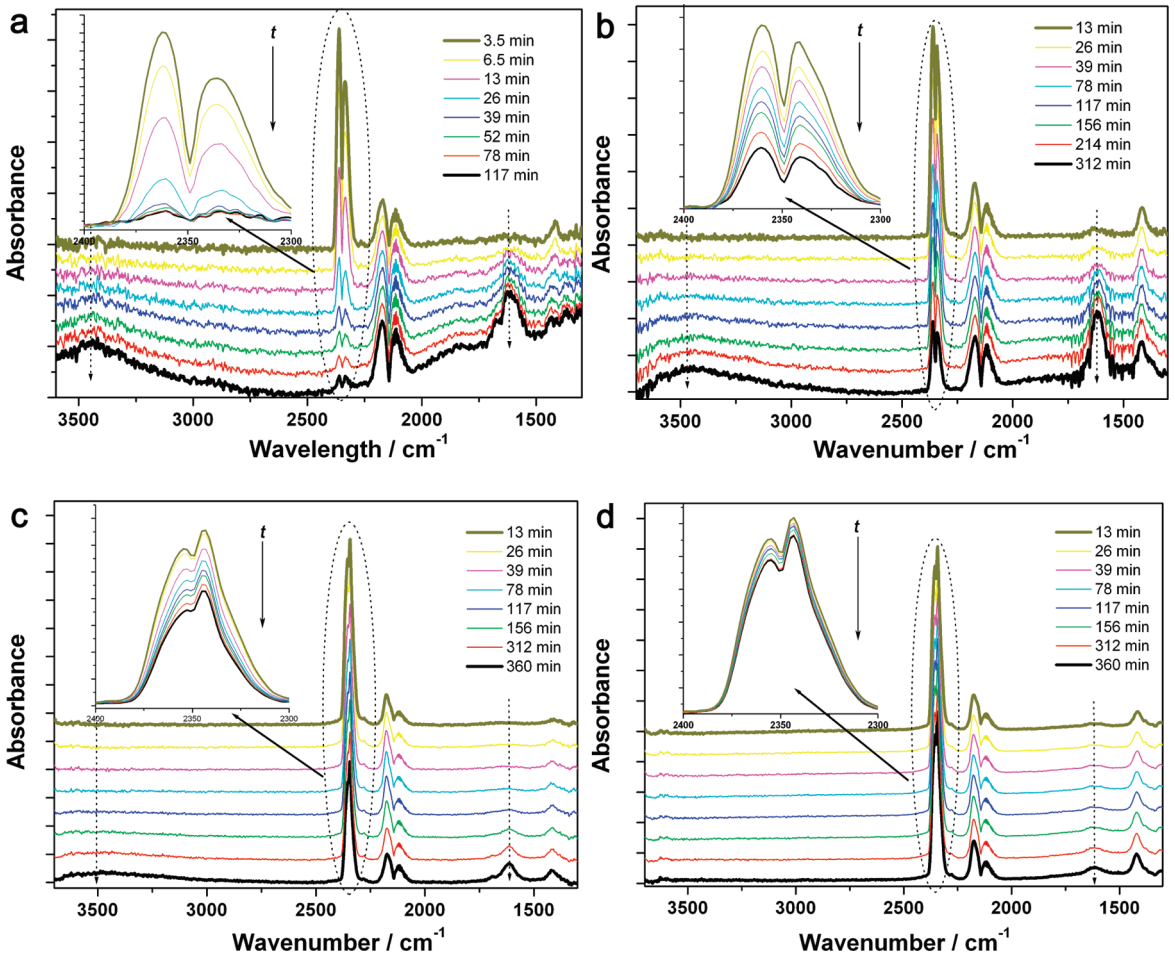

Figure 8. Sequence of in situ DRIFT spectra recorded during CO oxidation on Co_3O_4−SiO_2 catalyst at constant temperature of (a) 80, (b) 20, and (c) −25 °C under normal conditions and (d) −25 °C under dry conditions. (Insets) Enlarged details of the C−O stretch region characteristic for CO_2. Catalyst, 15 mg; reaction gas flow rate, 30 mL·min^{-1}.

about the evolution of reaction intermediates along with side products during CO oxidation at different temperatures. Figure 8 illustrates the evolution of the full spectra recorded with the Co_3O_4−SiO_2 catalyst during the reaction under normal conditions at temperatures of 80, 20, and −25 °C. The spectra reveal the characteristic gas-phase bands of CO at 2110 and 2170 cm^{-1} and of CO_2 at 2336 and 2360 cm^{-1}. A broad band at 3444 cm^{-1} has been assigned to the stretching vibration of adsorbed molecular H_2O on the catalyst.[36−38] A set of bands in the range 1300−1700 cm^{-1} was also observed, among which the band at 1614 cm^{-1} corresponds to the bending mode of adsorbed molecular H_2O,[36−38] while other bands are assigned to various vibrations of carbonates.[39] These general spectral features were similar for the catalyst at different temperatures, while the intensities of some bands as well as their evolution during reaction were appreciably different. This holds, for instance, for the CO_2 gas-phase band and the band assigned to the OH bending mode. The integrated intensity of the bands characteristic for gaseous CO_2 and that of adsorbed H_2O (bending mode at 1614 cm^{-1}) are plotted as a function of time in Figure 9. The band intensity of gaseous CO_2 is a measure for the catalyst activity. It can be seen that the catalyst deactivated with increasing temperature from −25 to 80 °C, which closely resembles the deactivation curve measured in the catalytic plug-flow reactor, as reported above. The increasing intensity of the band at 1614 cm^{-1} at the same time indicates increasing amounts of adsorbed water. This behavior supports the notion that adsorption of moisture from the feed gas is the origin of the fast deactivation of the Co_3O_4−SiO_2 composite catalyst in the intermediate-temperature regime. At even higher temperatures of 150 and 200 °C, the in situ DRIFT spectra during reaction (Figure S10, Supporting Information,) show that at these temperatures the water adsorption is largely suppressed; concurrently, no strong deactivation is observed, which is consistent with the temperature dependence of the activity as shown in Figure 4a.

For comparison, in situ DRIFT spectra were also measured under dry conditions. Figure 8d and Figure S11a,b (Supporting Information) show the spectra recorded under dry conditions. Compared with the results obtained under normal conditions, the accumulation of adsorbed H_2O was strongly suppressed, due to the much lower concentration of moisture in the feed gas. Correspondingly, the catalyst showed stable and high activity even after 360 min. However, some deactivation still occurred under these dry conditions, as shown in Figure S11c,d (Supporting Information), which became more severe with the increase in temperature from −25 to 20 and 80 °C (see the enlarged details of the CO_2 regions as insets), demonstrating that even very small amounts of moisture can affect the activity of the Co_3O_4−SiO_2

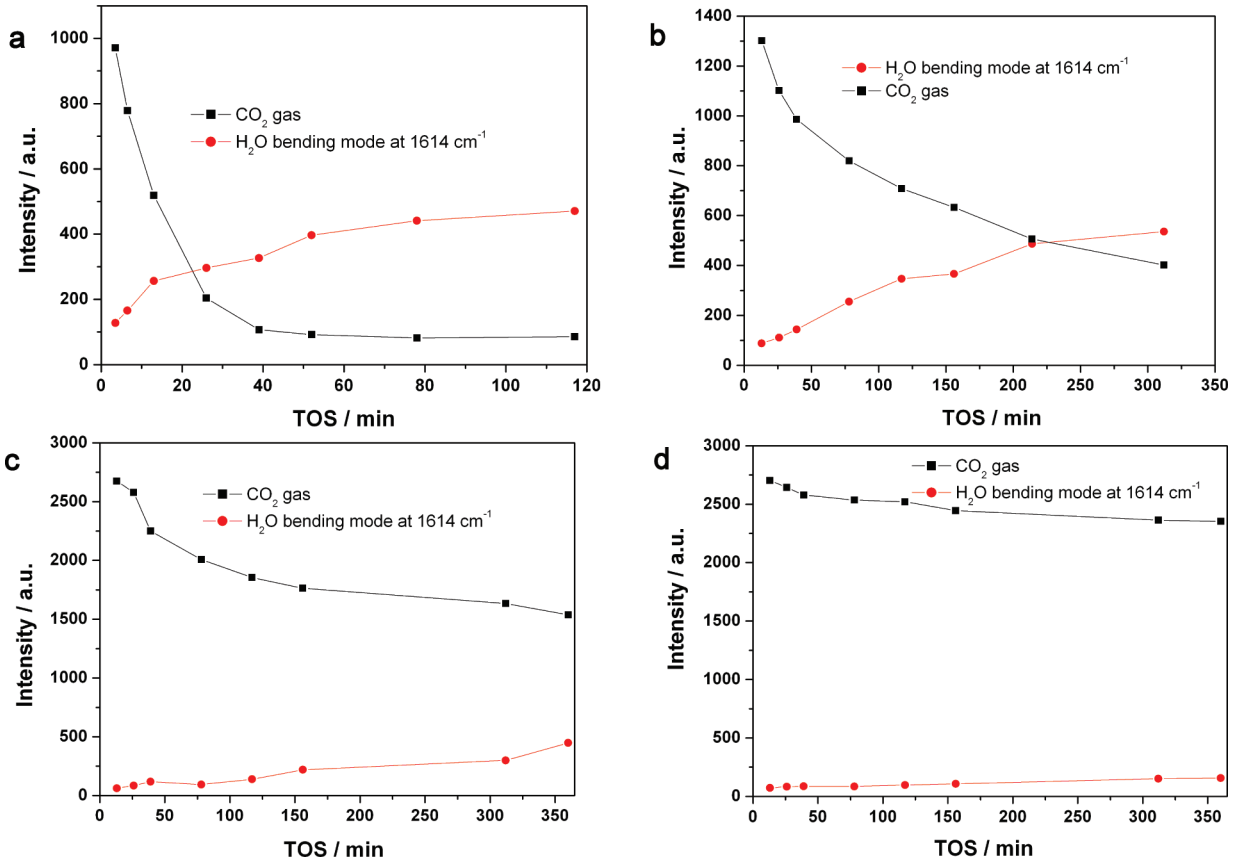

Figure 9. Evolution of DRIFT signals characteristic for H_2O adsorption (band of bending mode at 1614 cm^{-1}) and CO_2 as a function of time during CO oxidation at temperatures of (a) 80, (b) 20, and (c) −25 °C under normal conditions and (d) −25 °C under dry conditions.

catalyst. This influence of moisture was not observed for the $Au/Mg(OH)_2$ and Au/MgO catalysts mentioned above. In that case, the U-shaped conversion versus temperature profiles were observed under dry conditions as well as in gas streams containing higher concentrations of water. Thus, the unusual catalytic behavior indeed has a different origin as in the case of the Co_3O_4−SiO_2 composite.

The presence of SiO_2 in the catalyst clearly enhances the catalytic activity of the Co_3O_4. The activity maximum is observed for a Si/Co ratio of 0.5: pure Co_3O_4 is much less active, and pure SiO_2 does not show any activity in the temperature range investigated (Figure S12, Supporting Information). The mode by which the SiO_2 increases the activity is still unclear. The XRD and XPS data suggest that Co_3O_4 does not incorporate large fractions of SiO_2. However, the addition of SiO_2 can greatly influence the microstructure (including crystalline domain size of Co_3O_4, surface area, and dislocation density) of the Co_3O_4−SiO_2 composite, which can strongly affect the catalytic performance. Thus the increased activity could be due to cobalt sites with Si atoms in their vicinity. However, it could also be due to the strongly altered microstructure in the presence of SiO_2. The correlation between the structure/microstructure and the catalytic properties of these Co_3O_4−SiO_2 composite catalysts is currently under investigation in order to obtain more insight into the mode of action of the silica additive. The results of this study will be reported in a future publication.

CONCLUSION

We have prepared a small-sized Co_3O_4−SiO_2 nanocomposite catalyst, the surface of which is rich in silica and Co(II) species compared with normal Co_3O_4, and which exhibited very high activity for CO oxidation even at −76 °C and for extended times on stream. An unusual U-shaped curve of the temperature-dependent activity was observed under normal conditions, indicating negative apparent activation energies. However, under dry conditions, no such negative apparent activation energies were observed, and the catalyst showed much higher stability at both low and high temperatures. On the basis of extensive catalytic tests under various conditions and additional studies with in situ Raman and FTIR spectroscopy, we identified the adsorption of H_2O molecules on the surface of the catalyst as the origin of the negative apparent activation energies at intermediate temperatures under normal conditions.

ASSOCIATED CONTENT

Supporting Information. Twelve figures showing additional results on characterization and catalytic performance tests of Co_3O_4−SiO_2 nanocomposite catalysts. This material is available free of charge via the Internet at http://pubs.acs.org.

AUTHOR INFORMATION

Corresponding Author
schueth@mpi-muelheim.mpg.de

ACKNOWLEDGMENT

We thank Mr. H. Bongard and Mr. B. Spliethoff for the SEM and TEM measurements. Funding in addition to basic support by

the Max Planck Society was provided by SFB558 of DFG and the Alexander von Humboldt Foundation.

REFERENCES

(1) Haruta, M.; Tsubota, S.; Kobayashi, T.; Kageyama, H.; Genet, M. J.; Delmon, B. *J. Catal.* **1993**, *144*, 175–192.
(2) Yamaura, H.; Moriya, K.; Miura, N.; Yamazoe, N. *Sens. Actuators, B* **2000**, *65*, 39–41.
(3) Adams, K. M.; Graham, G. W. *Appl. Catal., B* **2008**, *80*, 343–352.
(4) Landon, P.; Ferguson, J.; Solsona, B. E.; Garcia, T.; Carley, A. F.; Herzing, A. A.; Kiely, C. J.; Golunski, S. E.; Hutchings, G. J. *Chem. Commun.* **2005**, 3385–3387.
(5) Haruta, M.; Kobayashi, T.; Sano, H.; Yamada, N. *Chem. Lett.* **1987**, 405–408.
(6) Cunningham, D. A. H.; Kobayashi, T.; Kamijo, N.; Haruta, M. *Catal. Lett.* **1994**, *25*, 257–264.
(7) Yu, Y. B.; Takei, T.; Ohashi, H.; He, H.; Zhang, X. L.; Haruta, M. *J. Catal.* **2009**, *267*, 121–128.
(8) Jansson, J. *J. Catal.* **2000**, *194*, 55–60.
(9) Jansson, J.; Skoglundh, M.; Fridell, E.; Thormahlen, P. *Top. Catal.* **2001**, *16*, 385–389.
(10) Jansson, J.; Palmqvist, A. E. C.; Fridell, E.; Skoglundh, M.; Osterlund, L.; Thormahlen, P.; Langer, V. *J. Catal.* **2002**, *211*, 387–397.
(11) Thormählen, P.; Skoglundh, M.; Fridell, E.; Andersson, B. *J. Catal.* **1999**, *188*, 300–310.
(12) Xie, X. W.; Li, Y.; Liu, Z. Q.; Haruta, M.; Shen, W. J. *Nature* **2009**, *458*, 746–749.
(13) Tüysüz, H.; Comotti, M.; Schüth, F. *Chem. Commun.* **2008**, 4022–4024.
(14) Schwickardi, M.; Johann, T.; Schmidt, W.; Schüth, F. *Chem. Mater.* **2002**, *14*, 3913–3919.
(15) Natile, M. M.; Glisenti, A. *Chem. Mater.* **2002**, *14*, 3090–3099.
(16) Grillo, F.; Natile, M. M.; Glisenti, A. *Appl. Catal., B* **2004**, *48*, 267–274.
(17) Saalfrank, J. W.; Maier, W. F. *Angew. Chem., Int. Ed.* **2004**, *43*, 2028–2031.
(18) Fortunato, G.; Oswald, H. R.; Reller, A. *J. Mater. Chem.* **2001**, *11*, 905–911.
(19) Date, M.; Okumura, M.; Tsubota, S.; Haruta, M. *Angew. Chem., Int. Ed.* **2004**, *43*, 2129–2132.
(20) Cunningham, D. A. H.; Vogel, W.; Haruta, M. *Catal. Lett.* **1999**, *63*, 43–47.
(21) Jia, C. J.; Liu, Y.; Bongard, H.; Schüth, F. *J. Am. Chem. Soc.* **2010**, *132*, 1520–1522.
(22) Schubert, M. M.; Hackenberg, S.; van Veen, A. C.; Muhler, M.; Plzak, V.; Behm, R. J. *J. Catal.* **2001**, *197*, 113–122.
(23) Haruta, M. *CATTECH* **2002**, *6*, 102–115.
(24) Guzman, J.; Carrettin, S.; Corma, A. *J. Am. Chem. Soc.* **2005**, *127*, 3286–3287.
(25) Guzman, J.; Carrettin, S.; Fierro-Gonzalez, J. C.; Hao, Y. L.; Gates, B. C.; Corma, A. *Angew. Chem., Int. Ed.* **2005**, *44*, 4778–4781.
(26) van Bokhoven, J. A.; Louis, C.; Miller, J.; Tromp, M.; Safonova, O. V.; Glatzel, P. *Angew. Chem., Int. Ed.* **2006**, *45*, 4651–4654.
(27) Giamello, E.; Sojka, Z.; Che, M.; Zecchina, A. *J. Phys. Chem.* **1986**, *90*, 6084–6091.
(28) Golodets, G .I. In *Heterogeneous Catalytic Reaction Involving Molecular Oxygen* ; Ross, J. R. H., Ed.; Studies in Surface Science and Catalysis, Vol. 15; Elsevier: Amsterdam—Oxford—New York, 1983; p 280.
(29) Berg, J. V. D.; Dillen, A. J. V.; Meijden, J. V. D.; Geus, J. W. *Surface Properties and Catalysis by Non-Metals*; Bonnelle, J. P., Delmon, B., Derouane, E., Eds.; D. Reidel Publishing Company: Dordrecht, The Netherlands, 1983; p 493.
(30) Ohtsuka, H.; Tabata, T.; Okada, O.; Sabatino, L. M. F.; Bellussi, G. *Catal. Lett.* **1997**, *44*, 265–270.
(31) Carrettin, S.; Hao, Y.; Aguilar-Guerrero, V.; Gates, B. C.; Trasobares, S.; Calvino, J. J.; Corma, A *Chem.—Eur. J.* **2007**, *13*, 7771–7779.
(32) Pushkarev, V. V.; Kovalchuk, V. I.; d'Itri, J. L. *J. Phys. Chem. B* **2004**, *108*, 5341–5348.
(33) Lide, D. R., Ed. *CRC Handbook of Chemistry and Physics*, 77th ed.; CRC Press: Boca Raton, FL, 1996—1997; pp 6—12.
(34) Boccuzzi, F.; Chiorino, A.; Manzoli, M.; Andreeva, D.; Tabakova, T *J. Catal.* **1999**, *188*, 176–185.
(35) Leppelt, R.; Schumacher, B.; Plzak, V.; Kinne, M.; Behm, R. J. *J. Catal.* **2006**, *244*, 137–152.
(36) Yates, D. J. C. *J. Phys. Chem.* **1961**, *65*, 746–753.
(37) Jones, P.; Hockey, J. A. *J. Chem. Soc., Faraday Trans.* **1972**, *68*, 907–913.
(38) Tanaka, K.; White, J. M. *J. Phys. Chem.* **1982**, *86*, 4708–4714.
(39) Schumacher, B.; Denkwitz, Y.; Plzak, V.; Kinne, M.; Behm, R. J. *J. Catal.* **2004**, *224*, 449–462.